RSC Advances

PAPER

View Article Online
View Journal | View Issue

Cite this: *RSC Adv.*, 2025, **15**, 18559

A twisted double donor in donor–acceptor–donor D_2–D_1–A–D_1–D_2 type emitters yields multicomponent charge-transfer emission†

Dovydas Blazevicius,[a] Gintare Krucaite,[a] Alla Bogoslovska,[b] Saulius Grigalevicius,[a] Amjad Ali,[cd] Hans Ågren,[de] Glib Baryshnikov[c] and Oleg Dimitriev *[b]

Received 23rd April 2025
Accepted 26th May 2025

DOI: 10.1039/d5ra02848e

rsc.li/rsc-advances

Complex donor arms in thermally-activated delay fluorescence (TADF) molecules can potentially provide additional options for charge-transfer (CT) emission through higher twisting disorder, leading to broader emission spectra. Here we design novel TADF emitters with double twisted donor moieties and show that a structural complication of the carbazole-based donor arms by changing the molecular structure from D–A–D to D_2–D_1–A–D_1–D_2 yields a transition from a dual to a triple emission band with an additional CT emission component, providing a corresponding red shift and increasing low-energy emission contribution. The revealed relationship between increased complexity of the donor moiety and the multicomponent CT emission band in the D–A–D structures provides a clue for design of TADF emitters with extended emission spectra.

Introduction

Emitters possessing thermally activated delayed fluorescence (TADF) are usually highly twisted molecules, where the twisting conformation provides several important properties that crucially impact photophysical properties of the TADF emitters themselves. First, a twisted molecular conformation is beneficial for the intramolecular charge transfer (CT) process that accompanies molecular excitation,[1] effectively separating the excited electron and hole on electron accepting and electron donating parts of the molecule, leading to corresponding separation of wave functions of the HOMO and the LUMO, respectively. This results in a reduced triplet-singlet gap ΔE_{ST} necessary for an effective reverse intersystem crossing (RISC) process. In this way, twisted conformation is favourable for reducing spatial overlap of molecular orbitals, which is useful for generation of additional channels to facilitate RISC.[2] Second, twisted molecular conformations, on one hand, increase steric hindrance that prevents intermolecular π–π stacking in solid films, which, on the other hand, is favorable for aggregation-induced emission properties in the solid state, since it also inhibits the vibrations and rotations of molecules, thus reducing non-radiative decays.[3]

In terms of the emission spectral shape, a twisted conformation of TADF molecules often provides a dual emission. Such emission can arise due to the combination of two different mechanisms such as fluorescence and phosphorescence, intra- and intermolecular CT or intramolecular CT originating from two asymmetric donor shoulders in the D–A–D molecular structure.[4] In this work, we study the origin of dual or multicomponent fluorescence due to a purely twisting mechanism that yields locally excited (LE) and CT states[5] or two CT states,[6] which are associated with the different twisting conformers. The different conformers can be either in the ground state or in the excited state, such as quasi-axial and quasi-equatorial ones[7] or extended and compact CT-induced conformations of the emitter.[8] The dual emission has been reported for different twisted D–A and D–A–D compounds, based on a simple-component donor moiety, such as phenothiazine (PTZ) derivative or its analogues (dihydrophenophosphanizine (DPPZS), 9,9-dimethyl-9,10-dihydroacridine (DMAC), PSeZ, *etc.*),[6,9–13] carbazole derivatives[14] and 5-acetaminoindole.[15] At the same time, the effect of additional twisting due to the complexity of donor moieties remains relatively unexplored. As an example, a synthesis of a D_2–D_1–A triad molecule with rigid coplanar carbazole (D_1) and twisted triphenylamine (D_2) has been reported, where a face-to-face alignment of D_2 and A was possible and gave the observed dual emission in solution, assigned to

[a]*Department of Polymer Chemistry and Technology, Kaunas University of Technology, Radvilenu Plentas 19, Kaunas, LT50254, Lithuania*

[b]*V. Lashkaryov Institute of Semiconductor Physics, NAS of Ukraine, Pr. Nauki 41, Kyiv 03028, Ukraine. E-mail: dimitr@isp.kiev.ua*

[c]*Laboratory of Organic Electronics and Wallenberg Wood Science Center, Linköping University, Norrköping 60174, Sweden*

[d]*Institute of Advanced Materials, Faculty of Chemistry, Wrocław University of Science and Technology, PL-50370 Wrocław, Poland*

[e]*Department of Physics and Astronomy, Uppsala University, Box 516, SE-751 20 Uppsala, Sweden*

† Electronic supplementary information (ESI) available: Experimental details and additional information. See DOI: https://doi.org/10.1039/d5ra02848e

intramolecular through-π conjugation CT emission from D_1 to A and intramolecular exciplex-like CT emission from D_2 to A.[16] Thus, increasing the twisting degrees of freedom is suggested to yield additional PL components and an emission spectrum that covers a broader visible range, which is useful for specific applications and design of white-light OLEDs.[6]

In this work, we designed a set of donor–acceptor–donor (D–A–D) emitters with the donor arm of increasing complexity (*i.e.*, D–D and D_1–D_2) that varies by twisting ability with respect to the acceptor core of pyrimidine, but which excludes exciplex formation due to the inability of a stacking conformation between D and A, in order to understand how the increasing twisting disorder influences the PL spectra. We found that the above structural complication of the donor arm yields a triple, *i.e.*, a three-component, PL emission band with corresponding red shift and increasing contribution of the low-energy components.

Results and discussion

A structural complication of the donor arm was realized by attaching to the first carbazole unit either a second carbazole to construct a D–D arm or triphenylamine to construct a D_1–D_2 arm (Fig. 1). A single bond between the two donor moieties in the arm allowed them to twist with respect to each other (Fig. 1). The additional moieties in the donor arms facilitated increasing conjugation length and decreasing bandgap (Fig. 2 and Table 1), together with separation of the HOMO and LUMO distributions in the compounds (Fig. 1). A separation of the HOMO and LUMO distribution is usually associated with increasing twisting between photoexcited donor and acceptor moieties, which, in turn, reduces the singlet–triplet bandgap in **2** and **3** (Table 1). It is interesting to note that the change in ΔE_{ST} is not smooth, that is, it remarkably decreases in **2**, but then increases in **3**, approaching that in **1**. Such behaviour correlates well with the changes in the dihedral angle between the pyrimidine and first carbazole moiety, where no change in the dihedral angle of specific arms was found upon photoexcitation for two conformers of **3** and one conformer of **1** (Fig. 1 and Table S1†); however, no correlation with respect to the twisting of the second donor moiety could be observed. The same trend was found in shifting the HOMO and LUMO levels. That is, both HOMO and LUMO energies remarkably decreased in **2** by about 0.5 eV with respect to **1**, but these increased again in **3**,

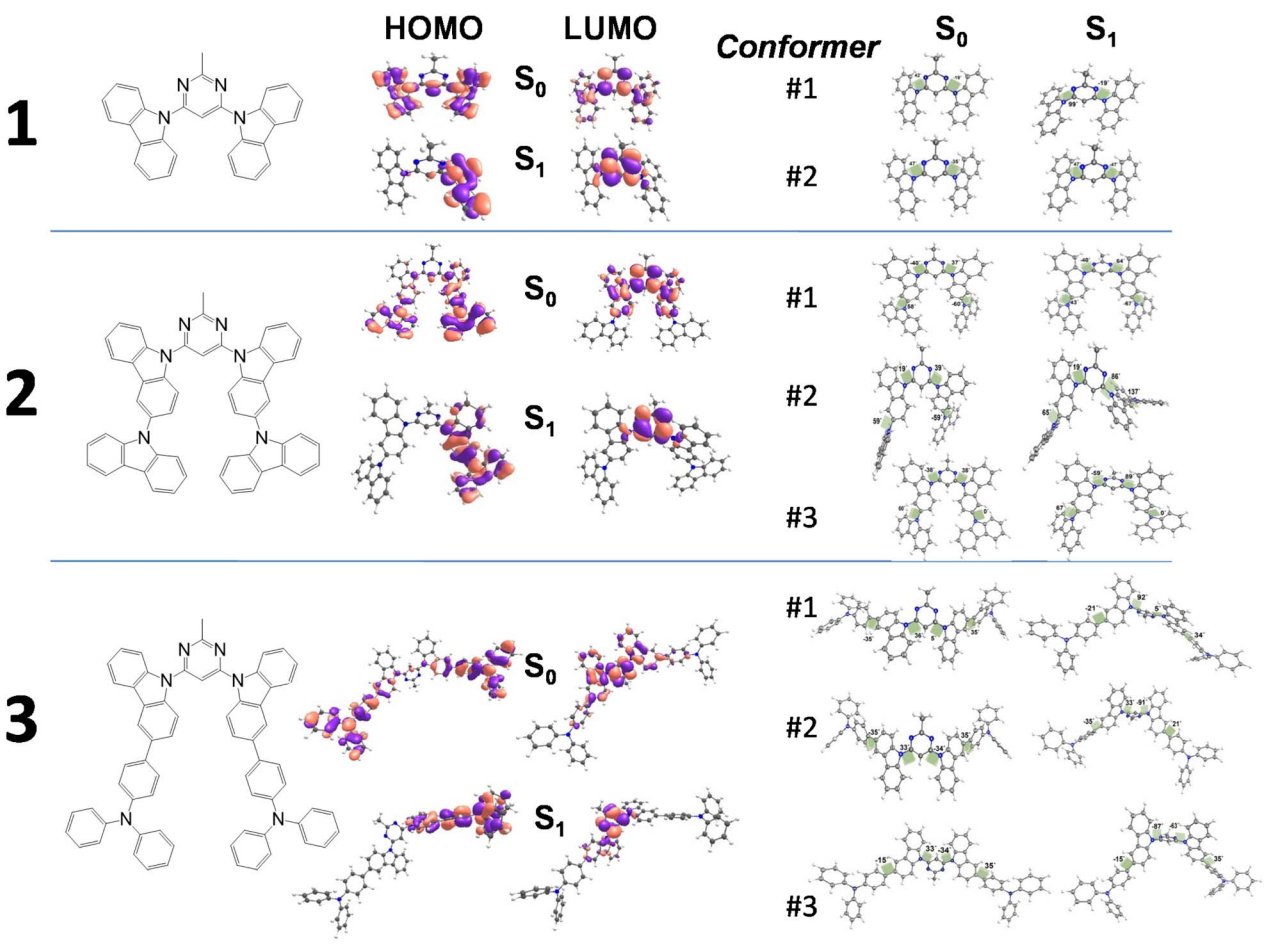

Fig. 1 Chemical structures, HOMO and LUMO map distributions, as well as ground-state and excited-state conformations of the compounds **1**–**3** calculated by TD-DFT using the B3LYP functional and the 6-31G(d,p) basis set in chloroform solvent. Dihedral angles between pyrimidine and carbazole (θ_1), as well as between the first and the second carbazole or carbazole and triphenylamine moieties (θ_2), are indicated (see also Table S1†).

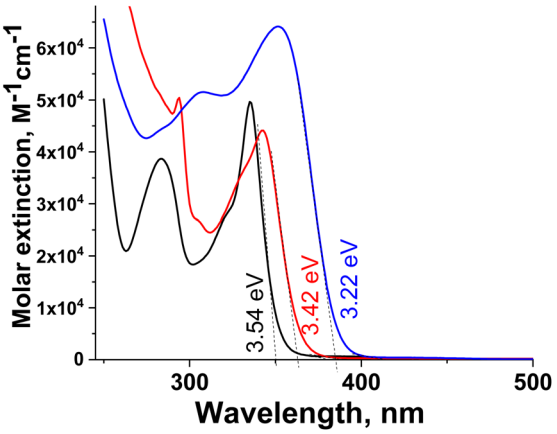

Fig. 2 UV-Vis spectra of chloroform solutions (10^{-5} M) of the compounds **1** (black), **2** (red), and **3** (blue). The bandgaps determined from the onset absorption are indicated.

approaching those in **1** (Table 1). Therefore, a tentative conclusion can be made that the twisting of the photoexcited donor unit just next to the acceptor one plays a dominant role in the behaviour of HOMO, LUMO, and triplet energy levels of the compounds.

The increasing extent of twisting freedom resulted in complication of the PL emission spectra as well, reflecting the coexisting of conformers with different twisting conformations. In the simplest case of the compound **1**, which contains two simple arms with a single carbazole moiety in the each arm, the PL spectrum revealed a dominant PL band near 410 nm for the toluene, chloroform and THF solutions and a 450 nm one for the acetone solution (Fig. 3), which is assigned to the locally excited (LE) and first charge-transfer (CT1) emission component, respectively. Here, the LE emission vanishes in the solution with relatively high polarity, *i.e.*, acetone, whereas a CT emission component is relatively small in low-polar solvents. Since LE emission is usually produced from a non-twisted or slightly twisted conformer, whereas CT emission from a highly twisted one, it can be concluded that the simultaneously observed LE and CT emissions can originate either from different conformers or the different arms of **1**, which possess no twisting and high twisting in the excited state compared to the ground state, respectively (Fig. 1).

When a second carbazole moiety is added to the donor arms in **2**, the former LE component near 410 nm can still be observed in non-polar toluene and low-polar THF as a shoulder; however, a CT1 emission component becomes developed, indicating a solvent-dependent maximum observed at 460, 468, and 478 nm for THF, chloroform, and acetone solution, respectively (Fig. 3). The rise of an additional PL component near 540 nm, denoted as CT2 emission, can be seen as well, which is increasing with increasing solvent polarity. The CT2 component becomes dominant in compound **3** (Fig. 3), where a second carbazole moiety in **2** is replaced by a triphenylamine one, strengthening the donor properties of the arm overall. Here, the CT2 emission is associated with additional conformers present in the solution due to the complexity of the donor arm, where a second donor moiety added facilitates increasing twisting disorder. Specifically, the CT2 emission component in **3** is red-shifted to *ca.* 550 nm, while the CT1 component is observed at 475, 485, and 490 nm for THF, chloroform, and acetone solution, respectively.

Comparison of PL emission spectra of **1**, **2**, and **3** in the same solvent further elucidates the difference related to the dye complexity (Fig. 4). Specifically, in non-polar toluene, the relative contribution of conformers with the LE emission dominates and in terms of the integral of the first Gaussian in the spectra of **1**, **2**, and **3** constitutes the ratio of 51 : 45 : 0, respectively. The relative contribution of conformers with the CT1 component increases as 27 : 33 : 47, respectively, whereas conformers with the CT2 component can be identified only in **3** (Table 2).

In THF, the relative contribution of the LE emission component to the spectra of **1**, **2**, and **3** constitutes 52 : 16 : 3, respectively. The ratio of the CT1 component is 16 : 80 : 78, and the CT2 component increases as 0 : 12 : 31, respectively. The compound **3** here possesses very small LE emission, while compound **1** lacks conformers with the CT2 emission.

In chloroform, the relative contribution of the LE emission component of **1**, **2**, and **3** decreases as 51 : 21 : 0, respectively. The relative contribution ratio of the CT1 component is 21 : 66 : 60, whereas the CT2 component increases as 0 : 59 : 78, respectively. That is, the compound **1** does not possess conformers with the CT2 emission, while the compound **3** lacks conformers with the LE emission.

In the more polar solvent acetone, the LE emission component was not found. Most probably, a highly twisted conformation forms according to the solvent polarity increase[17] or solvent-dependent structural relaxation.[18] The first emission component in **1** observed at 446 nm is assigned to CT1 because of its red shift and significant broadening compared to the LE emission (Table 2). The relative contribution ratio of the CT1

Table 1 Experimentally determined LUMO, HOMO, bandgap (E_g), Stokes shift (ΔE_S), and PLQY and computationally calculated by DFT singlet and triplet energy levels as well as a singlet–triplet bandgap (ΔE_{ST}) of the materials. For experimental and computational details, see ESI

Dye#	LUMO[a], eV	HOMO[b], eV	E_g[c], eV	ΔE_S[d], eV	PLQY[e]	S_1, eV	T_1, eV	ΔE_{ST}, eV
1	−1.96	−5.50	3.54	0.83	0.09	3.65	3.12	0.43
2	−2.48	−5.90	3.42	1.33	0.37	3.29	3.09	0.20
3	−2.23	−5.45	3.22	1.29	0.43	3.16	2.78	0.38

[a] Determined as HOMO plus E_g. [b] Determined by UPS (see Fig. S5). [c] See Fig. 2. [d] Chloroform solutions. [e] Toluene solutions.

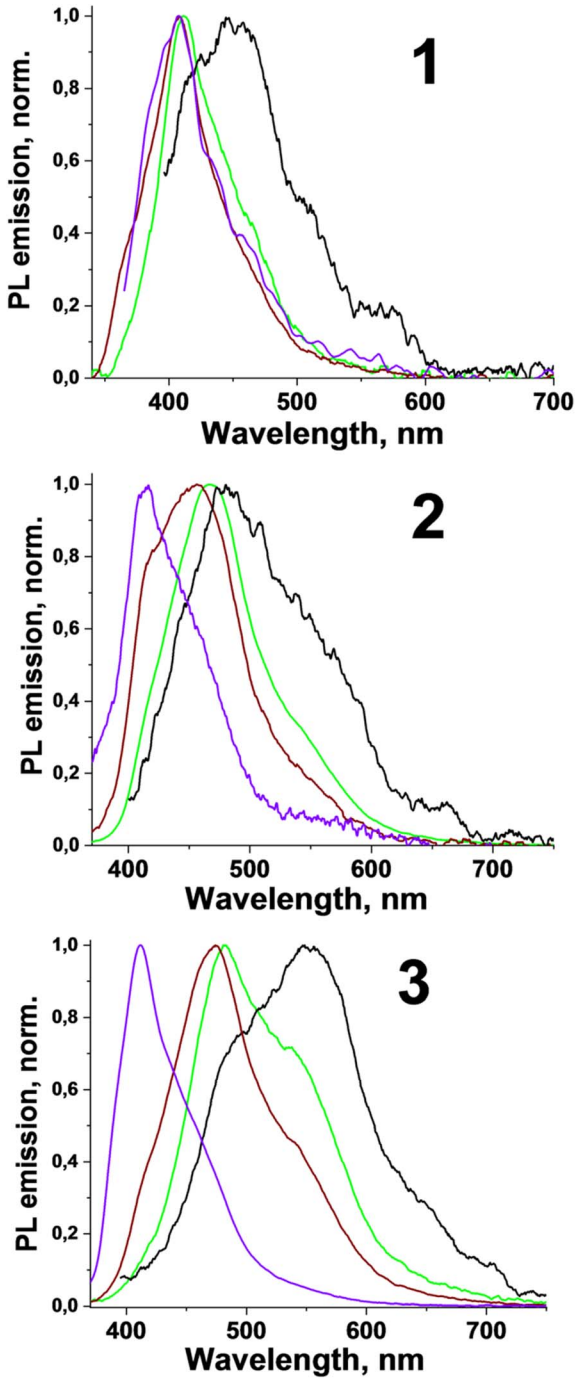

Fig. 3 PL emission spectra of the compounds **1**–**3** in toluene (violet), THF (brown), chloroform (green), and acetone (black) solutions (10^{-5} M).

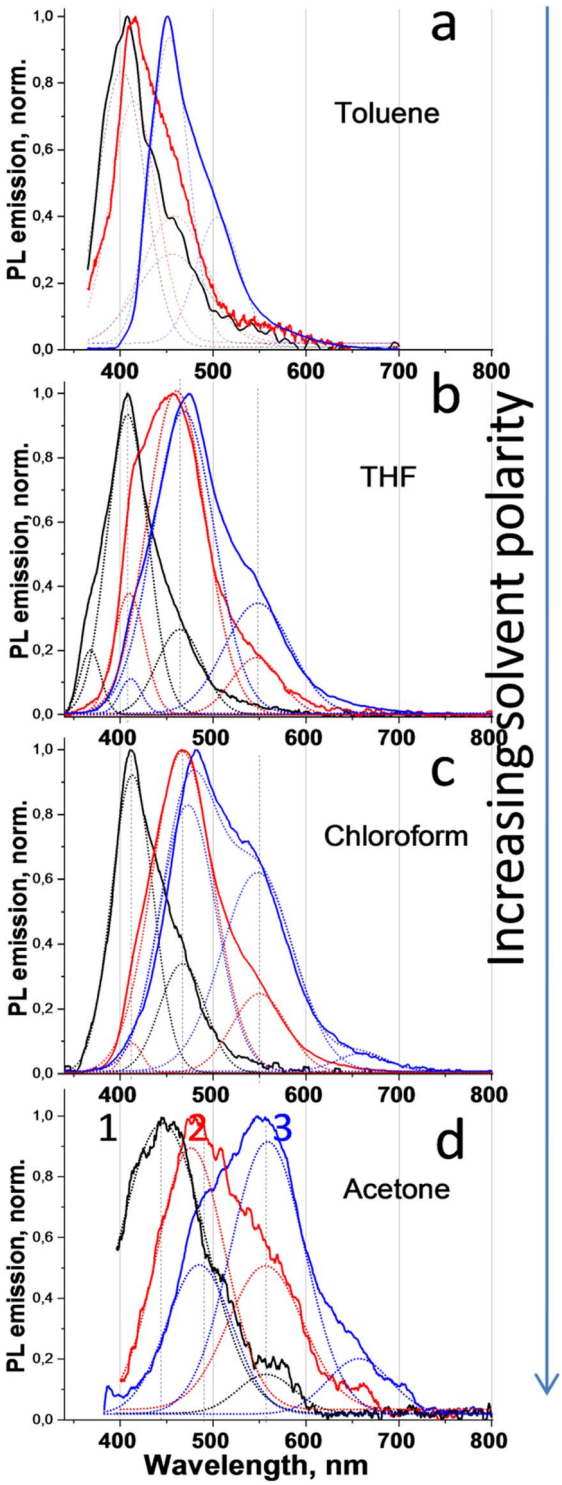

Fig. 4 PL emission spectra deconvoluted into Gaussians (shown by dotted curves) of **1** (black), **2** (red), and **3** (blue) of (a) toluene, (b) THF, (c) chloroform and (d) acetone solutions (all 10^{-5} M). λ_{exc} = 254 nm (b and c) and 365 nm (a and d).

emission to the spectra of **1**, **2**, and **3** in acetone decreases as 110 : 79 : 43, along with the shift of the CT1 emission maximum found at 446, 476, and 485 nm, respectively, whereas the CT2 component increases as 9 : 48 : 90. An additional component of unclear nature at 657 nm can be identified in the PL spectrum of **3** as well (Fig. 4).

The unambiguous proof of the CT character of the last two emission component refers to their solvent polarity dependence. The wavelength of the CT1 band increases from 453 to 485 nm as the relative solvent polarity increases from 0.099 to 0.355 (Fig. 5). An even steeper red shift with solvent polarity is observed for CT2, whose wavelength changes by

Table 2 Wavelength of the emission maximum, FWHM, and relative integral intensity of PL emission components of the compounds in different solvents, whose spectra are reduced to the same maximum (see Fig. 1)

	λ_{max}, nm			FWHM, cm^{-1}			Integral PL intensity, a.u.		
Dye #	LE	CT1	CT2	LE	CT1	CT2	LE	CT1	CT2
Toluene (relative polarity 0.099)									
1	402	456	—	3094	3703	—	52	27	—
2	414	458	—	2917	3289	—	45	33	—
3	—	453	505	—	1998	1843	—	47	22
THF (relative polarity 0.207)									
1	408	464	—	2643	2276	—	51	16	—
2	410	460	546	1963	2977	1778	16	80	12
3	411	468	548	1362	3010	2364	3	78	31
Chloroform (relative polarity 0.259)									
1	413	467	—	2640	2247	—	51	21	—
2	413	467	550	1231	3026	1950	21	66	59
3	—	473	549	—	2670	2570	—	60	78
Acetone (relative polarity 0.355)									
1	—	446	557	—	4646	1934	—	110	9
2	—	476	557	—	3222	2610	—	79	48
3	—	485	559	—	2976	2560	—	43	90

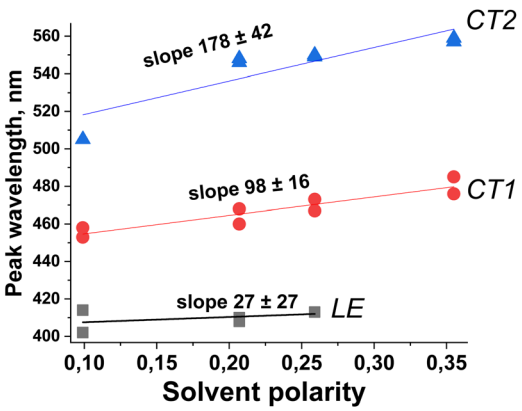

Fig. 5 Peak position of the Gaussian components of the PL emission spectra (see Table 2) as a function of the solvent polarity.

54 nm, *i.e.*, from 505 to 559 nm. At the same time, the spectral position of the LE emission component does not change with solvent polarity within experimental error, as expected (Fig. 5). Different behaviour of CT1 and CT2 emission bands with solvent polarity suggests that the photoinduced charge transfer occurs from the remote donor to acceptor unity for CT2, while it is locked at the acceptor unity next to the donor for CT1, producing different dipole moments stabilized by the polar solvent environment.

An additional evidence of the twisting disorder in compounds **1–3**, leading to multicomponent PL emission related to the coexistence of the different twisted conformers, was obtained by comparing PL spectra of the solutions, thin films of the neat dyes and composite films where the dye molecules were diluted in the amorphous ethyl cellulose (EC) polymer matrix. In the latter case, the rigid polymer matrix suppressed molecular twisting[19] upon photoexcitation in compounds **2** and **3**, resulting in predominant conformers with the LE band near 400 nm, which were thus mostly present in the matrix, whereas the neat dye films revealed spectral broadening with increasing FWHM by a factor of ~1.5, which can be deconvoluted into three Gaussians, indicating the mere presence of three conformers (Fig. 6). Thus, a clear difference in the PL spectral shapes of the neat and composite films and also solutions of **2** and **3** indicated that double donor groups in these compounds facilitate higher twisting disorder when being unrestricted from the rigid environment.

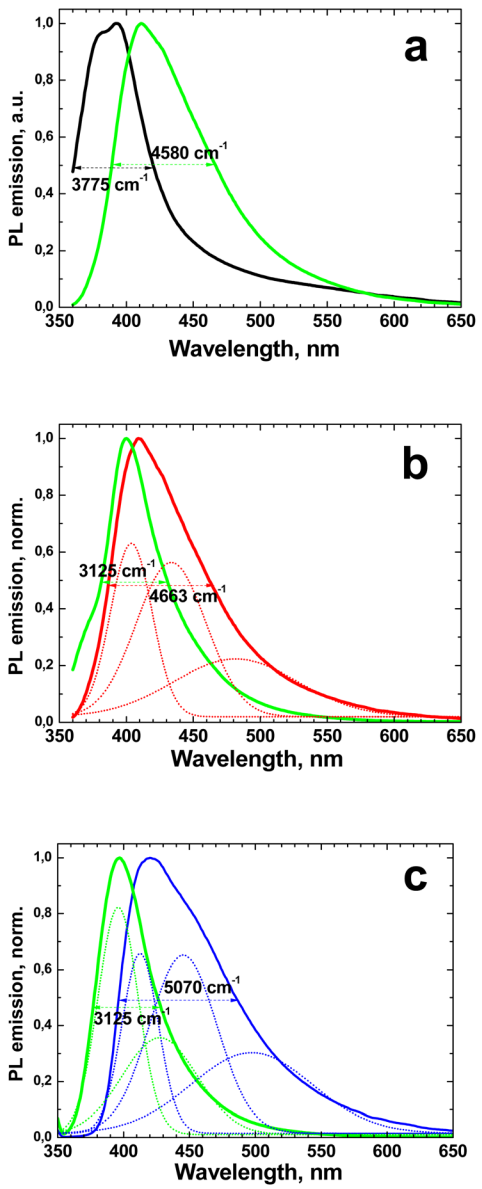

Fig. 6 PL spectra (λ_{exc} = 340 nm) of dyes in the EC matrix (green) and dye neat films of (a) **1**, (b) **2**, and (c) **3**.

The behaviour of compound **1** in the EC matrix was different. Since this molecule possesses poorer twisting behaviour, the EC matrix did not indicate a significant twisting suppression. Moreover, the dye neat films showed a relatively narrow PL emission band (Fig. 6a). It should be noted that the poor twisting of **1** makes it possible to form a crystalline structure of this compound in the solid films (Fig. S6†), whereas the EC matrix suppresses formation of the crystalline phase, leading to a broader PL emission band of amorphous structure.

Conclusions

Motivated by the general endeavour to find new design principles for improvement of TADF emitters, we explored in this work a set of donor–acceptor–donor emitters having a donor arm of increasing complexity that vary by its twisting ability with respect to the acceptor core. We can derive both detailed and general conclusions of this work: among the former we find that the CT1 and CT2 emission components mostly originate from the photoexcited charge transfer from the first donor (carbazole) moiety and the second donor (carbazole or triphenylamine) moiety, respectively, with respect to the acceptor (pyrimidine). The wavelength of the CT1 emission component varies between 446 and 485 nm depending on the availability of the second donor moiety in the D arm and on the solvent polarity as well. The origin of the CT2 emission component is assigned to the longer CT passway in the conjugated structure rather than to a steeper molecular twisting. For example, no larger twisting of the carbazole unit with respect to the acceptor one was found upon addition of a second donor unit (Fig. 1). The longer CT passway results in a red shift of the CT2 emission that varies between 546 and 557 nm and it also depends on the solvent polarity. No CT2 emission could be observed in **1** since no additional donor moiety is available in this dye structure, whereas the relative intensity of the CT2 emission increases when the triphenylamine moiety added in **3** compared to the second carbazole moiety added in **2** (Table 2), which is consistent with the fact that triphenylamine derivatives are considered to be among the strongest electron donor materials for solar cells.[20]

As a general conclusion we find that the complication of the donor arm in the twisted D–A–D compounds leads to increasing twisting disorder and, as a consequence, to the appearance of additional charge-transfer routes from the different donor moieties. This is verified by the appearance of additional emission components and broadening of the PL spectra. The observed relationship between the complexity of the donor moiety and multicomponent CT emission band in the D–A–D structures suggests new design principles of thermally activated delayed fluorescence emitters with controllable emission properties.

Data availability

The data supporting this article have been included as part of the ESI.†

Author contributions

D. B., G. K., and A. A.: investigation, resources, software; A. B.: investigation, S. G.: writing – original drafts, review & editing; H. Å. and G. B.: project management, review & editing; O. D.: methodology, investigation, writing – original drafts, review & editing. All authors have read and agreed to the published version of the manuscript.

Conflicts of interest

There are no conflicts to declare.

Acknowledgements

This work was financially supported by the Research Council of Lithuania (Grant No. S-LU-24-7) and Ministry of Education and Science of Ukraine (project M/54-2024) and in part by the Knut and Alice Wallenberg Foundation (KAW) through the Wallenberg Wood Science Center. G. B. is thankful for support from the Swedish Research Council (starting grant no. 2020-04600) and from the European Union (ERC, LUMOR, 101077649). A. A. and H. Å. are thankful for support from the Polish National Science Centre, (within the NCN OPUS 26 research project no. UMO-2023/51/B/ST5/00677). Part of the quantum-chemical calculations were carried out using computational resources provided by the National Academic Infrastructure for Supercomputing in Sweden (NAISS 2025-5-140) at the National Supercomputer Centre (NSC), Linköping University, partially funded by the Swedish Research Council (grant no. 2022-06725). Additional calculations were performed at the Wrocław Center for Networking and Supercomputing (WCSS).

Notes and references

1 Z. R. Grabowski, K. Rotkiewicz and W. Rettig, *Chem. Rev.*, 2003, **103**, 3899–4032.
2 Z. He, J. Li, D. Liu, H. Wan, Y. Mei and C. Shi, *J. Mater. Chem. C*, 2022, **10**, 18189–18199.
3 T. Zhang, Y. Xiao, H. Wang, S. Kong, R. Huang, V. Ka-Man Au, T. Yu and W. Huang, *Angew Chem. Int. Ed. Engl.*, 2023, **62**, e202301896.
4 X. Li, S. Shen, C. Zhang, M. Liu, J. Lu and L. Zhu, *Sci. China Chem.*, 2021, **64**, 534–546.
5 N. Acar, J. Kurzawa, N. Fritz, A. Stockmann, C. Roman, S. Schneider and T. Clark, *J. Phys. Chem. A*, 2003, **107**, 9530–9541.
6 X. Tian, S. Xiao, J. Sun, J. Yan, G. Li, B. Zhao, Y. Miao, L. Wang, H. Wang and D. Ma, *Chem. Eng. J.*, 2024, **485**, 149692.
7 X. Y. Lauteslager, I. H. M. van Stokkum, H. J. van Ramesdonk, A. M. Brouwer and J. W. Verhoeven, *J. Phys. Chem. A*, 1999, **103**, 653–659.
8 A. Stockmann, J. Kurzawa, N. Fritz, N. Acar, S. Schneider, J. Daub, R. Engl and T. Clark, *J. Phys. Chem. A*, 2002, **106**, 7958–7970.

9 K. Wang, Y.-Z. Shi, C.-J. Zheng, W. Liu, K. Liang, X. Li, M. Zhang, H. Lin, S.-L. Tao, C.-S. Lee, X.-M. Ou and X.-H. Zhang, *ACS Appl. Mater. Interfaces*, 2018, **10**, 31515–31525.
10 H. Tanaka, K. Shizu, H. Nakanotani and C. Adachi, *J. Phys. Chem. C Nanomater. Interfaces*, 2014, **118**, 15985–15994.
11 Y. Takeda, T. Kaihara, M. Okazaki, H. Higginbotham, P. Data, N. Tohnai and S. Minakata, *Chem. Commun.*, 2018, **54**, 6847–6850.
12 D. de Sa Pereira, D. R. Lee, N. A. Kukhta, K. H. Lee, C. L. Kim, A. S. Batsanov, J. Y. Lee and A. P. Monkman, *J. Mater. Chem. C*, 2019, **7**, 10481–10490.
13 W. Li, X. Cai, B. Li, L. Gan, Y. He, K. Liu, D. Chen, Y.-C. Wu and S.-J. Su, *Angew. Chem.*, 2019, **131**, 592–596.
14 Y. Geng, A. D'Aleo, K. Inada, L.-S. Cui, J. U. Kim, H. Nakanotani and C. Adachi, *Angew. Chem.*, 2017, **129**, 16763–16767.
15 X. Li, G. Baryshnikov, C. Deng, X. Bao, B. Wu, Y. Zhou, H. Ågren and L. Zhu, *Nat. Commun.*, 2019, **10**, 1–9.
16 J.-A. Lin, S.-W. Li, Z.-Y. Liu, D.-G. Chen, C.-Y. Huang, Y.-C. Wei, Y.-Y. Chen, Z.-H. Tsai, C.-Y. Lo, W.-Y. Hung, K.-T. Wong and P.-T. Chou, *Chem. Mater.*, 2019, **31**, 5981–5992.
17 L. A. Rodríguez-Cortés, F. J. Hernández, M. Rodríguez, R. A. Toscano, A. Jiménez-Sánchez, R. Crespo-Otero and B. Rodríguez-Molina, *Matter*, 2023, **6**, 1140–1159.
18 T. Ryu, K. Miyata, M. Saigo, Y. Shimoda, Y. Tsuchiya, H. Nakanotani, C. Adachi and K. Onda, *Chem. Phys. Lett.*, 2022, **809**, 140155.
19 D. Tavgeniene, G. Krucaite, D. Blazevicius, S. Grigalevicius, A. Bogoslovska, A. Ali, G. Baryshnikov, P. Smertenko, M. Fahlman, A. Smertenko and O. Dimitriev, *Opt. Mater.*, 2025, **165**, 117097.
20 M. Bélières, V. Sartor, P.-L. Fabre, R. Poteau, G. Bordeau and N. Chouini-Lalanne, *Dyes Pigm.*, 2018, **153**, 275–283.